





Article

Analysis of the Wall Geometry with Different Strategies for High Deposition Wire Arc Additive Manufacturing of Mild Steel

Eider Aldalur ¹, Fernando Veiga ^{1,*}, Alfredo Suárez ¹, Jon Bilbao ² and Aitzol Lamikiz ³

¹ TECNALIA, Basque Research and Technology Alliance (BRTA), Parque Científico y Tecnológico de Gipuzkoa, E20009 Donostia-San Sebastián, Spain; eider.aldalur@tecnalia.com (E.A.); alfredo.suarez@tecnalia.com (A.S.)

² ADDILAN Fabricación Aditiva S.L., Eguzkitza 1, 48200 Durango, Spain; jbilbao@addilan.com

³ Department of Mechanical Engineering, University of the Basque Country (UPV/EHU), E48013 Bilbao, Spain; aitzol.lamikiz@ehu.eus

* Correspondence: fernando.veiga@tecnalia.com; Tel.: +34-902-760-000

Received: 31 May 2020; Accepted: 3 July 2020; Published: 4 July 2020



Abstract: Additive manufacturing has gained relevance in recent decades as an alternative to the manufacture of metal parts. Among the additive technologies, those that are classified as Directed Energy Deposition (DED) are characterized by their high deposition rate, noticeably, Wire Arc Additive Manufacturing (WAAM). However, having the inability to produce parts with acceptable final surface quality and high geometric precision is to be considered an important disadvantage in this process. In this paper, different torch trajectory strategies (oscillatory motion and overlap) in the fabrication of low carbon steel walls will be compared using Gas Metal Arc Welding (GMAW)-based WAAM technology. The comparison is done with a study of the mechanical and microstructural characteristics of the produced walls and finally, addressing the productivity obtained utilizing each strategy. The oscillation strategy shows better results, regarding the utilization rate of deposited material and the flatness of the upper surface, this being advantageous for subsequent machining steps.

Keywords: additive Manufacturing; WAAM; GMAW; high deposition rate; mild steel; low carbon steel; oscillation strategy

1. Introduction

Additive Manufacturing (AM) is a new production concept that has generated increasing interest over the last ten years. A transformation has been promoted in the way that structurally complex parts can be manufactured with unrivaled design freedom [1]. Each AM technology consists of a particular combination of a heat source, feedstock and motion system, making it suitable for numerous applications. According to the standard terminology for AM by ASTM (ASTM F2792), AM technologies for metal components have been classified into four categories, one being the Directed Energy Deposition (DED) [2].

DED by definition is “an additive manufacturing process in which focused thermal energy is used to fuse materials by melting as they are being deposited” [3]. Amongst the DED technologies are wire-feed processes and powder-feed processes [4]. The ability to use wire as a feedstock, compared to powder, offers a reduction in price per kilogram and a high material usage efficiency. Therefore, the manufacture of large parts is ideal for the technologies that use wire as a feedstock, being the most effective additive processes for this purpose [5]. Furthermore, in these technologies no use of powder recycling systems is necessary, so a more environmentally friendly process is achieved. All these characteristics enable easier manipulation of material, thus reducing the safety and health concerns [6,7].

Wire Arc Additive Manufacturing (WAAM) is a wire-feed DED process that has become an interesting alternative for the manufacturing of low-medium complexity large parts due to its high deposition rate. WAAM capitalizes on the possibility to automate bead-deposition parameters [8]. The entire automatization process includes the power source, the torch movement, depending on the machine configuration, and the wire feeder. The possibility of establishing control over the deposition process and the trajectory during the deposition of the material, has given rise to the analysis of different trajectories for thick walls production. Xu et al. [9] have covered the analysis of three strategies: seven overlapped passes, square oscillation and triangular oscillation. Furthermore, heat accumulation analysis on the oscillating strategies is introduced. The heat accumulation in weaving welding is described in more detail in the work done by Chen et al. [10].

Within the known WAAM technologies, the most extended are Gas Metal Arc Welding (GMAW), Gas Tungsten Arc Welding (GTAW) and Plasma Arc Welding (PAW). This paper is focused on the study of the GMAW-Pulse process where the material (the wire) is melted due to the arc created between the wire and the top surface of the substrate material where the melt pool is formatted. In this process, CMT (Cold Metal Transfer), short-circuit transfer (SCT) or Pulse are some of the possible working modes defined by the current generation procedure [6,11,12]. The main advantages of GMAW are based on relatively inexpensive equipment, the ability to apply it to a wide range of metals, easy automatization and high deposition rates. Therefore, in order to obtain high deposition rates, it is necessary to maintain high wire feed speeds which can create instability in the process, with subsequent surface undulation. Owing to this, this parameter must be controlled in order to achieve admissible surface finish and maintain the required tolerance of the deposited part [8]. Notwithstanding, after completing the deposition by GMAW, final machining is always necessary to achieve the required geometrical tolerances.

Focusing on the search for the best parameter solution to obtain optimal geometry, some studies are presented. The analysis of the bead geometry parameters (bead width, bead height, penetration, and wetting angle) is made based on the welding parameters, such as wire feed speed, travel speed, current and shielding gas flow rate based on statistical methods by Dinovitzer et al. [13]. Meanwhile, Rios et al. [14] focus on the shape of the bead rather than on its dimensions, developing an analytical model for its estimation based on the parameters used. These geometries are characterized by having a parabola shape. The improvement of the final wall geometry is one of the greater challenges in WAAM technology.

For this aim, this research proposes to compare oscillating and overlapping additive manufacturing strategies with the objective to analyze the optimal strategy for generating a wall as close as possible to the target wall in terms of geometry, while meeting the requirements for mechanical properties. For the oscillating strategy, the novelty of this paper is given by the implementation of a high frequency triangular oscillation that makes it possible to obtain more homogeneous and flattened geometries that will then be easier to machine. Furthermore, in the previous literature, a triangular oscillation strategy with such a short wavelength and with such high deposition rates has not been studied from the point of view of geometry [15]. This new strategy can be used to manufacture parts more efficiently and productively and subsequent machining will be facilitated, obtaining geometries closer to the target geometry. Finally, this article presents the integration of a GMAW-PULS welding system with the possibility of an oscillating strategy in a Gantry machine manufactured specifically for the WAAM technology, which is new on the market.

In this paper, first, the means used to manufacture the parts and the tests carried out on them are presented. Then, the results are divided into productivity and growth per layer aspects. After, the comparison of the mechanical behavior of the final parts is made and finally, considerations on the geometry of the final parts, depending on the selected strategy, are analyzed. The results revealed that the oscillating path parameterization method is as capable of producing the final geometry as the more commonly implemented overlapping strategy. Thus, it helps to to make the trajectories more

flexible in the generation of parts with more complex geometries that could be undertaken with a more continuous (oscillatory) strategy than multiple discrete trajectories (overlapping).

2. Materials and Methods

2.1. Material and Set-Up

An Addilan (Durang, Spain) WAAM 3 axis AM machine equipped with a tilt table (+2-axis) and an inert-atmosphere close chamber was used to manufacture two walls; one with each strategy, one overlapping and the other oscillating. This specific closed build chamber is imperative to work with titanium or aluminum and other reactive materials. Although the technology chosen to carry out the work presented in this paper was the GMAW, due to the versatility of this AM machine, other processes, such as GTAW or PAW, were allowed. The GMAW process was based on the melting of the material with an electric arc created between the wire and the part. The energy generated by this electric arc was used to melt the material that was deposited on the top of the substrate and generated wall growth layer by layer. The build envelope for manufacturing parts was 1300 mm × 900 mm × 500 mm with a maximum weight of 300 kg. The additive manufacturing system was equipped with: a MIG/MAG welding power source, Titan XQ 400 AC puls, and a wire feeder, M drive 4 Rob5 XR RE, as the GMAW system (EWM, Mündersbach, Germany). Figure 1 shows a montage of the sensors used; a compact pyrometer Optris (Optris GmbH, Berlin, Germany) and a laser scanner, QuellTech Q4 (QuellTech, München, Germany), which were placed on the torch holder. At every two layers, the laser scanner recorded a cloud of points that reproduced the transversal geometry of the walls used to monitor the geometry of the deposited layers. The pyrometer was directed to the melted pool and it was used to determine cooling time. The cooling time is a non-productive period necessary between layers in order to promote the correct growth of the bead, without causing the collapse of the wall due to excess heat that melts the wall material. A personal computer was used to load the welding parameters and monitor them during the process. Finally, the data was sent to a database to be accessible remotely.

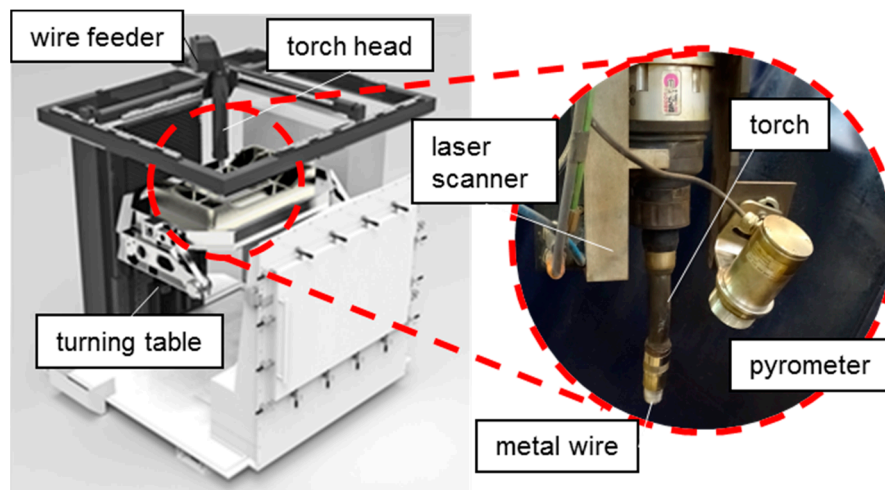


Figure 1. Addilan Additive Manufacturing (AM) machine; the welding torch equipped with a geometrical laser scanner and a pyrometer.

The wire material used for GMAW manufacturing of the walls in both strategies was ER70S-6 mild steel (DIN 8559SG2). The composition of ER70S-6 has been provided by the supplier in weight %: Mn-1.64, Si-0.94, C-0.06, Cr-0.02, Cu-0.02, Ni-0.02, S-0.016, P-0.013, Mo-0.005, Ti-0.004, Zr-0.002, Fe-bal. The diameter of the wire d_{wire} , to be used as raw material, was 1.2 mm. The substrate plate was S235JR steel (DIN ST37-2) in sheet form with a thickness of 8 mm.

2.2. Deposition Strategy and Metal Transfer Mode

This section describes the two strategies used for conducting tests. One wall has been fabricated in each strategy. The walls' dimensions were l : 220 mm long straight walls with the same w : width (20 mm) and z : height (70 mm). Figure 2 corresponds to the programmed path on the machine axis in both strategies. The first strategy used sought to cover 20 mm in width by overlapping three beads with a rate of 65% (6.9 mm) of the expected width of one single weld pass. The second strategy consisted of an oscillatory triangular movement of the torch. The peak to peak amplitude of the oscillation was 20 mm, which was compensated with a tool offset equal to half of the width of the expected weld pass, and a frequency of 1.5 Hz. In both walls, prior to the return trajectory, a dwell time was waited until the pyrometer read a temperature lower than 400 °C, to make the deposition over a solidified material. Therefore, in the oscillated strategy, a unique dwell time between layers was expected, and, in the overlapped strategy, one dwell time at each bead with a total of three per layer. In both strategies, the return trajectories ran in the opposite direction (starting from the other side of the weld pass) to compensate for the geometry of the welding pass. This decompensation was created due to the starts and stops of the process. On the other hand, thanks to the laser scanner, at every two layers a geometry of the walls has been represented to manually determine the Z position for the next layer trajectory on both strategies. Lasers installed on the machine gave a total amount of 244 points per profile and one profile each 2 mm. The transfer mode selected was the MAG-PULS.

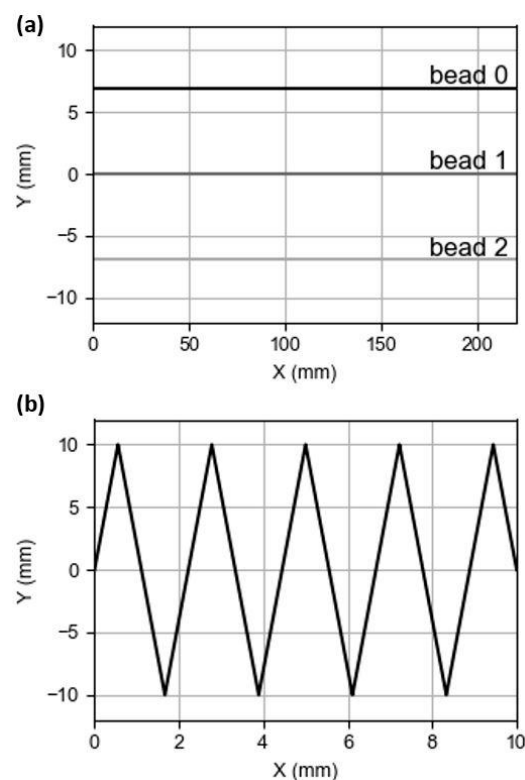


Figure 2. (a) Path of the overlapping strategy; (b) Path of the oscillatory strategy.

Within the variants of GMAW, the synergic pulsed GMAW (MIG/MAG) was selected. This working mode is one of the most used these days due to its operating method, which consists of unit current pulses digitally controlled from the power source. This provides identical droplet formation of molten material with a predetermined volume correlated to the electrode wire [16]. The synergic pulsed GMAW's main advantage is to be able to ensure stable burn off of the wire. Figure 3 shows the signal gathered from the power source during drop formation with an OROS data acquisition system (OROS GmbH, Koblenz, Germany) at 12.8 kHz frequency. The current rose with a controlled slope

until it reached the peak current in which the droplet was formed, this current fell, making a stop in an intermediate current for a short period of time until it reached the base current, in which the drop released. The period of the wave was 7.23 msec, which made a droplet deposition frequency of 138.2 Hz. The current parameters were established automatically through the power source database based on the wire speed, shielding gas, diameter and material of the electrode. The selected parameters were: steel, 80/20 Argon CO₂ shielding gas, wire diameter of 1.2 mm and wire feed speed of 8 m/min.

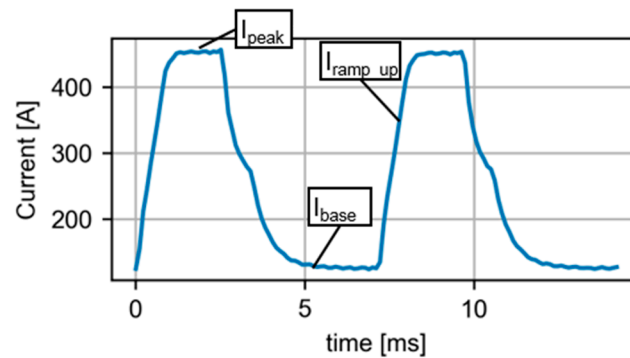


Figure 3. Current wave during drop formation on Gas Metal Arc Welding (GMAW).

Figure 3 shows the signal acquired from the power source for mild steel deposition with a wire feed speed of 8 m/min, common in both strategies. As it was a pulsed signal, each of the peak-to-base steps produced a drop. Therefore, the energy necessary to produce each drop can be considered constant in both strategies. From now on it will be considered that the number of drops defines the energy deposited in the parts. Furthermore, the following Figure 4 shows the average current and voltage per wall pass. It was observed that they are comparable in both strategies, therefore its product that defines the energy was equal in both cases.

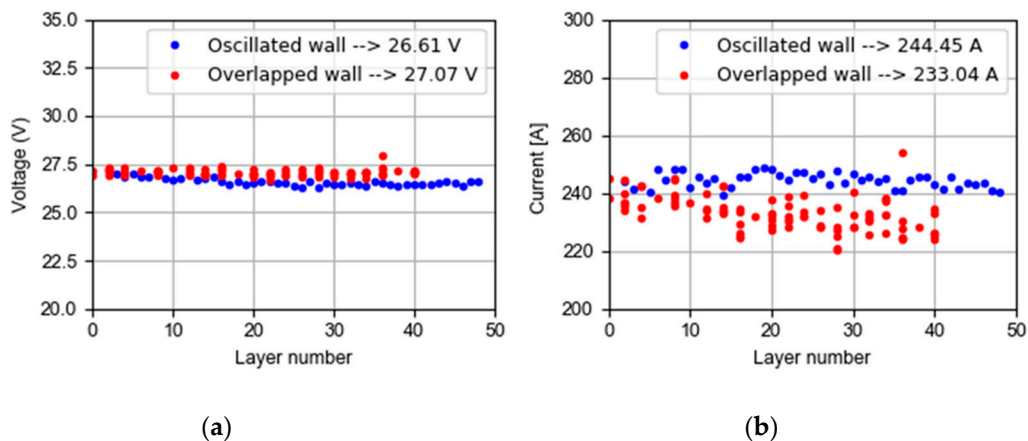


Figure 4. Mean current (a) and voltage (b) during additive manufacturing of each layer.

2.3. Preliminary Study for Parameters Selection

A preliminary study for parameter selection was carried out, designing a test battery in order to find the optimal process parameters to manufacture the walls. In this test battery, unitary beads were manufactured and scanned with a laser scanner. To design the preliminary experiment, within the range of possible wire feed speeds, 5 levels were chosen and a full factorial was completed, taking three levels of travel speed, as can be seen in Table 1.

Table 1. Test battery of GMAW-PULS in ER70.

Factors	Units	Coded Value				
		-2	-1	0	+1	+2
Wire feed speed (WFS)	[m/min]	4	6	8	10	12
Travel speed (TS)	[cm/min]	-	30	65	100	-

After the manufacture of the beads, these have been analyzed, taking into account the homogeneity, continuity, geometrical shape, penetration and dilution. To determine the penetration and dilution, macrographs of the transversal face of the beads were analyzed. Regarding the geometrical shape, to measure the width and height of the beads, the laser scanner results were utilized obtaining images, such as Figure 5a.

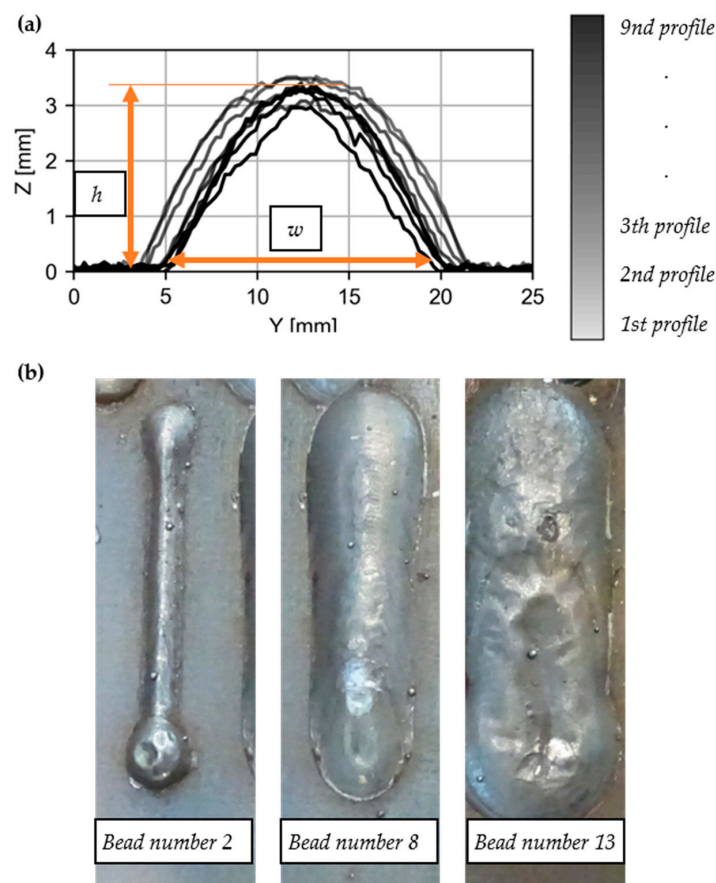


Figure 5. (a) Profiles acquired using the laser scanner in the bead 7, where the height (h) and width (w) can be seen; (b) Images of beads 2, 8 and 13.

Nine of the profiles generated by the laser in each scan have been acquired to obtain a cloud of points that reproduces the transversal geometry of each bead (Figure 5a). The width and height of the beads were calculated from each of these profiles and the average of these values (w_{avg} and h_{avg}) can be found in Table 2. Furthermore, in Table 2, the product of the inverse of the standard deviations of height and width can be seen. This inverse value is a geometrical feature (GF). The GF indicates the level of homogeneity and continuity of the beads and it was achieved following the Equation (1):

$$GF = \frac{\left(\frac{1}{\sigma_w} * \frac{1}{\sigma_h}\right)}{2} \quad (1)$$

where,

$$\sigma_w = \frac{\sqrt{\sum_{i=1}^n (w_i - \bar{w})^2}}{n}$$

$$\sigma_h = \frac{\sqrt{\sum_{i=1}^n (h_i - \bar{h})^2}}{n}$$

In addition, a wetting angle value can be found in Table 2 calculated as Equation (2):

$$\text{Wetting angle} = \tan^{-1}\left(\frac{h_{avg}}{w_{avg}/2}\right) \quad (2)$$

Table 2. Measurement results of the beads' geometry.

Beads Number	WFR	TS	Wavg (mm)	Havg (mm)	GF	Wetting Angle (°)
1	-2	-1	7.30	2.69	12.27	36.37
2	-2	0	4.62	1.69	49.45	36.19
3	-2	+1			Non-continuous	
4	-1	-1	11.28	2.91	8.23	27.29
5	-1	0	7.96	2.41	18.14	31.15
6	-1	+1	4.43	2.18	34.32	44.59
7	0	-1	15.26	2.98	8.22	21.34
8	0	0	7.88	2.25	63.50	29.73
9	0	+1	5.52	1.95	15.65	35.21
10	+1	-1	15.05	3.39	29.40	24.25
11	+1	0	8.73	2.93	11.21	33.89
12	+1	+1	7.69	2.63	25.51	34.39
13	+2	-1	17.21	4.19	6.86	25.94
14	+2	0	10.88	3.24	27.58	30.78
15	+2	+1	8.38	2.60	10.33	31.86

Once all the beads were measured employing the laser, the optimal welding parameters were determined, taking into account the maximum GF value and a desirable wetting angle [13]. In previous literature, it has been documented that a desirable wetting angle for additive manufacturing processes is 30°. Therefore, it was decided that the parameters used in bead 8 are the optimal ones.

After the characterization of the optimal welding parameters, the selected ones can be seen in Table 3. The resulting speeds to cover the wall length of the walls were comparable, as can be seen in the subsequent kinetic analysis. In this analysis, if the length of the path to cover the 200 mm in the X direction of the target wall was compared in the overlapped strategy, the torch ran 627.6 mm (3 mm × 200 mm of each welding pass and idle movement) and 200 mm in the case of oscillation. If we take into account the command traverse speeds (65 cm/min for overlapping and 20 cm/min for oscillating strategy), the addition time was comparable in both cases (1 min). The same wire feed lead to an equal deposition rate.

Table 3. Welding parameters for each wall.

Process Parameter	Overlapped Wall	Oscillated Wall
Wire feed speed [m/min]	8	8
Deposition rate [kg/h]	4.26	4.26
Torch speed [cm/min]	65	20
Stick-out [mm]	15	15
Shielding gas type	20% CO2-80% Ar	20% CO2-80% Ar
Gas flow [L/min]	17	17

2.4. Mechanical and Microstructural Characterization Method

The walls manufactured by GMAW-based WAAM using both strategies were analyzed. In addition, an analysis of the microstructure of the material was performed and mechanical tests were carried out: the tensile test and the Charpy test.

For the mechanical characterization of both walls, six tensile specimens were extracted in the vertical direction, six tensile specimens in the horizontal direction and four vertical specimens for the Charpy Impact test. Furthermore, another three samples in each wall were utilized to analyse the microstructure and the hardness. Figure 6 shows the arrangement of the specimens on the additive wall. We had the cylindrical specimens for tensile testing and rectangular pieces for the Charpy test. The arrangement of the specimens sought to analyze the influence of the directionality of the material on its mechanical behavior.

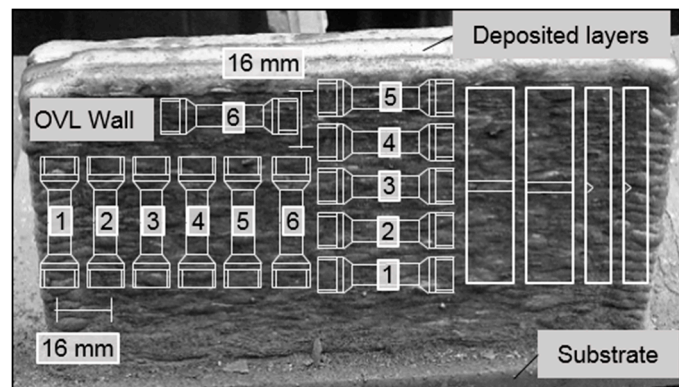


Figure 6. Arrangement of specimens for the mechanical properties analysis in both walls.

Wire Arc Additive Manufacturing showed anisotropy on the macrographic structure (disposition on the wall inner surface) due to the adding of material layer-by-layer. As can be seen in Figure 7, the arrangement of the layers was different in the case of oscillatory and overlapping strategies. The presence of inter-layer boundaries in the case of oscillation were observed since each layer was formed by a single bead, and in the case of the three overlapping beads that form each layer, inter-bead boundaries were noticed. The existence of an interface between the overlapping weld passes meant that there was less continuity inside the wall. To analyze the grain structure, Salmi et al. [17] present remarkable results using ultrasonic burnishing that increases hardness and quality on the surface compared with the typical post-processing techniques. Although these results are promising, in this paper, metallographic samples were extracted by conventional milling from the inner surface of the additive manufactured walls. Then, the specimens were mechanically polished and finally etched with a solution of 2% Nital-Nitric and Ethanol acid to reveal the grain structure, as suggested by MacKenzie [18]. In addition, hardness testing (Vickers hardness) was performed on the same samples at room temperature using a Struers Duramin A-300 machine (Struers, Ballerup, Denmark).

Therefore, the selection of specimens on different orientations on the wall was done. The dimensions of the tensile specimens followed the standard ISO 6892-1 [19], with a narrow diameter of 4 mm and a length of 22 mm, with threads at the ends of M-6. The machine where the uniaxial tensile tests were performed at room temperature was the Instron 5585H, with a maximum load of 100 kN and equipped with a contact extensometer, Instron EX2620-602 (Instron, Norwood, MA, USA). Charpy tests were performed at room temperature on an impact test pendulum Ibertest PIB300 machine (S.A.E. Ibertest, Madrid, Spain). Following standard ISO 148-1, Charpy impact test specimens with a 55 mm length and 10 mm thickness were used. The specimens were selected in the vertical direction from both walls.

A measurement of the geometry of both walls was addressed by means of the volumetric reconstruction of the profiles acquired in each layer. This measurement was made by means of the laser scanner installed and attached to the torch shown in Figure 1.

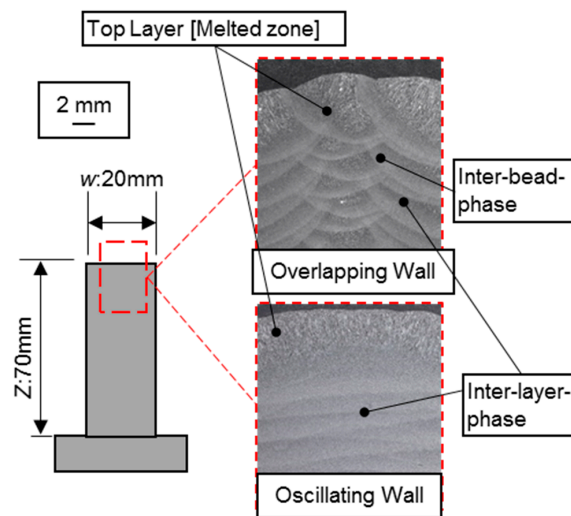


Figure 7. Macrography analysis of the layers disposal at the top of the walls in both strategies.

3. Results and Discussion

3.1. Process Characterization

To determine the heat input effect on the manufactured walls, it is important, first of all, to understand the process kinetics. In the case of the overlapped wall, the travel speed is constant throughout all the trajectory, resulting in a uniform deposition. On the other hand, a cycle of the torch trajectory in the oscillated wall and its travel speed distribution is shown in Figure 8. In this case, the speed is lower on the sides than in the central part, becoming null in the corners due to the change of direction. Thus, the material deposition is non-uniform along the entire path.

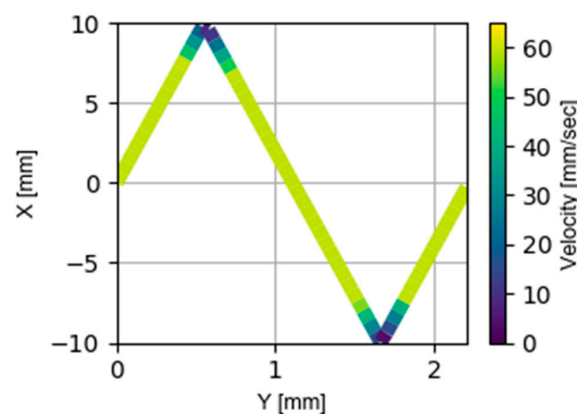


Figure 8. Torch trajectory and velocity during the oscillated wall manufacturing.

To obtain the number of drops per advanced millimeter, it would be sufficient to integrate the product of the instantaneous speed and the advance travelled in the x and y direction. In the case of overlap, it should be taken into account that it is necessary to overlap three weld passes to travel the same distance and that the instantaneous speed is constant and equal to the torch speed (T_s) (Equation (3)). In the case of oscillation, starting from the instantaneous speed as a function of the position of the torch registered in the control ($V(x, y)$), it is multiplied by the differential advance. In both cases, the droplet deposition frequency is given by the values of the power source with the selected transfer mode ($f = 138.2$ drops/sec). In Equation (4), the integration has been calculated by

means of its resolution based on the sum of the instantaneous speeds and positions registered in the monitoring system.

$$N_{drop_{ovl}} = V \cdot \Delta x \cdot \Delta y \quad (3)$$

$$N_{drop_{osc}} = \int_{-10}^{10} \int_0^1 V(x, y) \delta x \delta y \cdot f_{drop} \quad (4)$$

Table 4 below shows the comparison of droplets deposited per advanced millimeter in both torch movement strategies. In the case of oscillatory movement, a greater number of drops per advanced mm is observed with a more homogeneous distribution, according to the trajectory, as shown in Figure 8.

Table 4. Deposited number of drops per advanced millimeter in overlapping and oscillating strategies.

Strategy	Ndrops [drops/mm]
Overlapped wall	38.25
Oscillated wall	41.25

In addition to the drop transfer analysis, Figure 9 shows the instantaneous deposition energy calculated as the product of the current and the voltage divided by the speed of the torch. This deposition energy is constant in the case of the overlapping strategy and it is variable due to the kinetics of the process on the oscillation strategy, as shown in Figure 8.

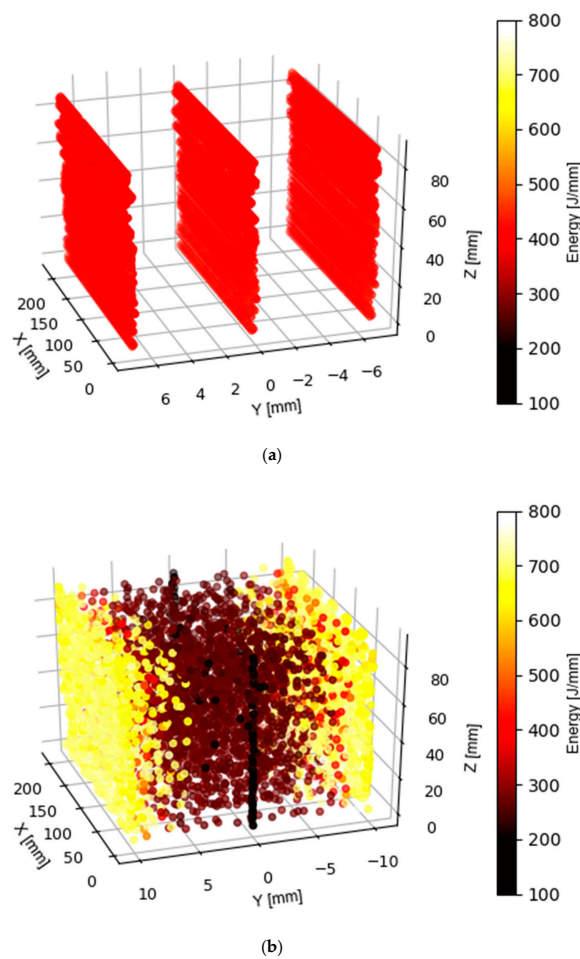


Figure 9. Deposition Energy during wall manufactured under (a) overlapping strategy and (b) oscillating strategy.

In order to ensure that the motion system has completed what was programmed in the manufacturing of the oscillated wall, Figure 10 presents the generated bead in the first layer. The width of the bead is slightly less than 20 mm of the target wall, because in layer 0 the substrate is cold and there is greater growth in the Z direction and a slight decrease in width.

The marks appreciated in Figure 10 are generated due to the oscillatory path and, by measuring the distance between two consecutive marks, the actual wavelength of the process can be determined. Five marks of the first bead are bordered by a red box (Figure 10) and the luminance values of the bordered part of the photo are analyzed, determining that the actual wavelength is 2.30 mm. Therefore, as the theoretical programmed wavelength was 2.22 mm, it can be concluded that the actual trajectory is in accordance with the programmed one. The complete zigzag shape is not observed on the top surface of the bead, since the theoretical programmed wavelength value is small, without producing marks on the forward side direction because they are removed by the next movement.

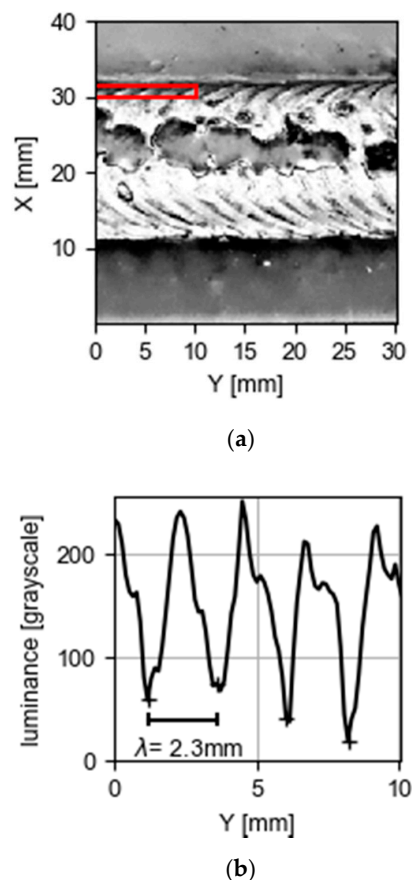


Figure 10. (a) Wavy-shaped track generated in the first deposited bead due to the wavelength of the oscillatory path. Note that five marks are in a red box; (b) Luminance values of the part of the photo bordered by the red box.

To highlight this point, Figure 11 presents the evolution of Z, the measured height of the wall along both strategies. It can be observed in the first layers that growth is greater in the oscillated wall than in the overlapped wall because at the beginning the substrate is at atmospheric temperature and the energy input and cooling times are not yet stable. After these first layers, the overlapped wall presents greater growth than in the oscillated wall, and the number of layers necessary to obtain the desired height is therefore reduced, 40 layers and 48 layers, respectively. The incidence of a more concentrated heat in the oscillatory strategy produces a greater dilution in this case, therefore a greater number of layers is necessary for the same growth in the Z direction.

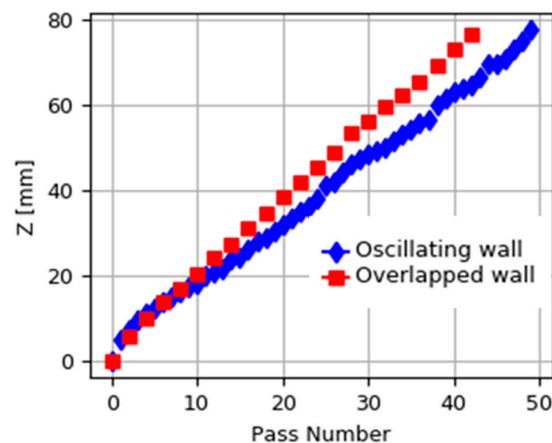


Figure 11. Wall height Z measured at layer growth evolution in both walls.

The manufacturing time is calculated as a summation of the adding time and the idle time, which considers the time to cool down the material between layers and non-productive movements. Figure 12 shows the surface temperatures of the welding pass during the addition and the idle time on both oscillating and overlapping strategies. The summation of the three intralayer times on the overlapping strategy supposes a longer run time than the interlayer time after manufacturing with an oscillatory strategy. The manufacturing time is longer in the case of the overlapping strategy (2 h 2 min) compared to values of the oscillating strategy (1 h 25 min). The main differences appear when idle time is compared, since three start–stop cycles must be done on the overlapping strategy. The idle time is 1 h 15 min for overlapping and 32 min for the oscillating strategy. On the other hand, overlapping adding time is more productive, reaching a value of 46 min as traverse speed is faster than the oscillating strategy. Adding time using an oscillating strategy is 52 min.

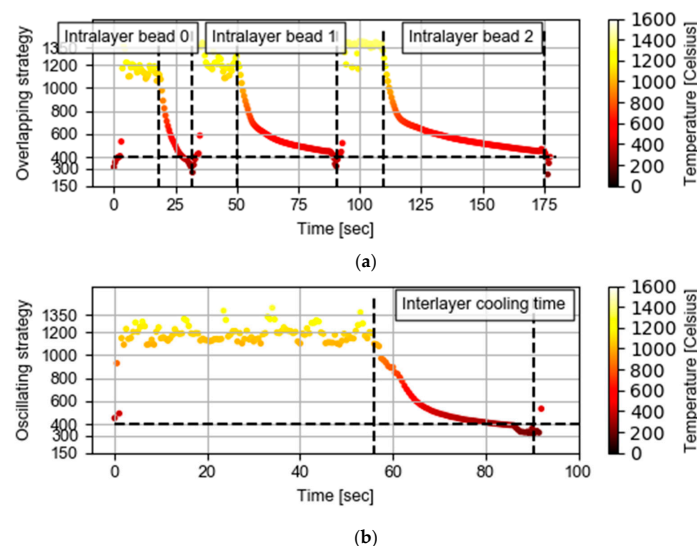


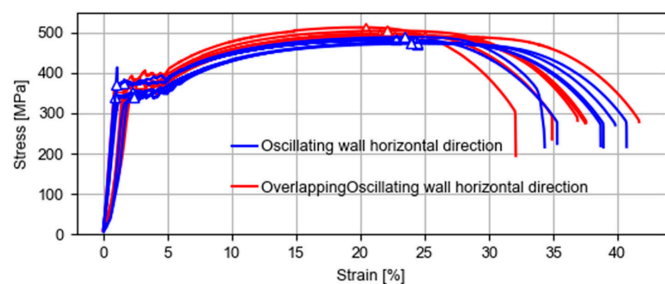
Figure 12. Temperature at the surface of the wall during one layer deposited in (a) overlapping strategy and (b) oscillating strategy.

3.2. Mechanical Characterization

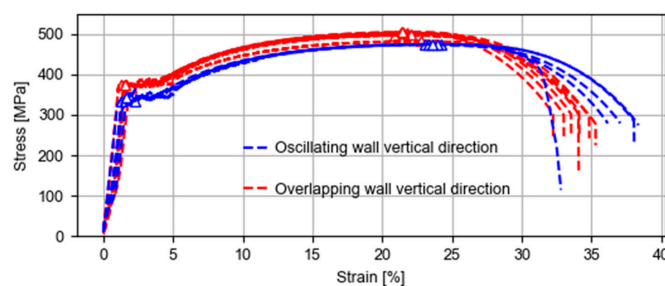
This section shows the mechanical results obtained from the wall test produced by overlapping and by oscillatory strategies. It is well known that solidification defects that may appear in WAAM samples, for example, porosity, lack of fusion, localized brittle zones, and grain coarsening in the heat-affected zones, can promote scatter in mechanical properties [20]. In Figure 13, the stress–strain curves of each test sample are represented. In the obtained values, some scatter is appreciated,

especially in elongation. It has been shown that, depending on the thermal history of each area, location-dependent mechanical properties are obtained [21]. As can be seen in Figure 6, six horizontal and six vertical tensile test specimens are cut from the walls. The results show slightly higher ultimate tensile strength (UTS) and yield strength (YS) values in the case of overlapping strategy, especially in the case of tests in the vertical direction.

Table 5 summarizes the results of the mechanical testing of the oscillating and overlapping walls. The standard deviation in the results of UTS and YS in the horizontal direction are greater than those observed in the vertical direction, as can already be seen in Figure 13. Charpy tests have been performed in order to analyze the influence of the bead direction on the fracture toughness. Although, in the literature [22,23] results on Charpy testing show larger scatter than the tensile test results in low carbon steels, which is created due to the different microstructures that can be seen throughout the part, for example the acicular ferrite lead to superior impact toughness results than polygonal ferrite [24], in the present study, the impact test results are similar in the two compared walls. On the other hand, Vickers hardness testing has been also performed at these walls. As it was pointed out by Salmi et al. [17] the samples extraction procedure can affect the obtained hardness values. Average values observed in the overlapping strategy are similar to the ones observed in the oscillating strategy. Results are similar to those addressed by [15] and slightly inferior to those reported by the wire supplier for this material as welded.



(a)



(b)

Figure 13. The stress–strain curve and ultimate tensile strength (UTS), yield strength (YS) and elongation percentage (Elong.) calculation on each test specimen in (a) horizontal direction and (b) vertical direction.

Table 5. Summary comparison of mechanical characterization on the overlapping and oscillating walls.

Sample	Direction	Tensile Test			Vickers Test	Charpy Impact Test
		UTS (MPa)	YS 0.2% (MPa)	Elong (%)	Hardness [HV]	Fracture Toughness (J)
Overlapped wall	Horizontal	498 ± 9	368 ± 12	36 ± 4	151 ± 9	193 ± 6
	Vertical	501 ± 3	368 ± 4	32 ± 1		
Oscillated wall	Horizontal	478 ± 6	354 ± 13	38 ± 3	142 ± 9	195 ± 4
	Vertical	474 ± 1	338 ± 4	36 ± 2		
ER70 as welded	-	500–640	>420	28	-	160

3.3. Analysis of the Wall Geometry

In this section, the final geometry of the manufactured wall is analyzed utilizing the different strategies of deposition: oscillatory strategy and overlapping of linear welds. The flatness as it is defined by [ASME Y14.5 standard] “specifies a tolerance zone defined by two parallel planes within which the surface must lie”, having been calculated as the difference between the major distance to mean value and the minor distance to the height on the upper surface of the wall.

Figure 14 shows the point cloud that is defined by each of the profile readings made by the laser. The two envelope lines that define the maximum profile and, above all, the minimum usable profile, are also shown. Lastly, the mean profile line between these two envelopes is shown. As can be seen, the flatness observed in the case of the use of an oscillatory strategy is greater than that of overlapping. The profile presented by the oscillation case is parabolic. Therefore, the material flows towards the central zone from the edges of the bead, even though, as shown in Table 4, a greater number of drops are deposited in that zone. This indicates that the material flows backward and upwards into the melt pool in the limit zone, going to the hot zone and avoiding the greater surface tension in the limit zone. The same effect was reported by Ma et al. [25], obtaining a flatter layer with a weaving strategy. This behavior observed in GMAW is different from that modeled for the case of PAW by the authors, Bai et al. [26], in which it was discovered that metal liquid flow was upward inside and outward on the surface.

Regarding the shape observed in the upper layer, it is observed that the wall obtained by means of oscillatory strategy is quasi-symmetrical, due to the nature of the movement of the torch and the movement of the metal in a fluid state. In contrast, in the case of the overlapping strategy, it can be seen how the growth of the lateral welds is less than that of the central weld due to the anisotropic configuration of the wall once each of the welds is manufactured. The production of a wall with a homogeneous top surface is critical for the subsequent face milling process and obtaining the finished wall. In previous works, Veiga et al. [27] have shown how face milling is a more critical machining process in this type of wall than tangential milling.

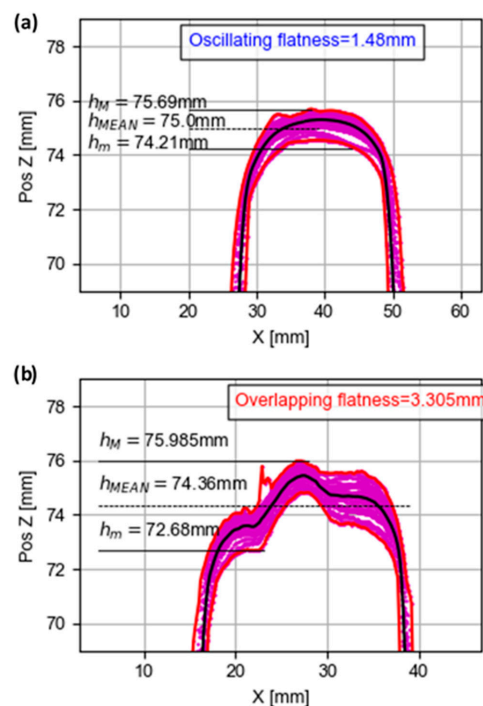


Figure 14. Transversal sections and determination of the flatness in the final piece for the wall manufactured by (a) oscillatory and (b) overlapping strategies.

The dimensions of the final wall will be determined by the minimum measured profile, shown in Figure 15, of the parabolic nature of the measured profiles; an effective wall of the rectangular cross-sectional area could be obtained. This cross-sectional area is of variable character depending on the effective height and width in which the target square is inscribed. In Figure 15, the effective cross-sectional area in both strategies is shown in red for the target width of 20 mm. The maximum effective height at which a wall of this height would be obtained would be greater in the case of an oscillatory strategy, this height being 72.2 mm compared to the 71.3 mm height observed in the case of walls obtained by overlapping. Although this difference is not very large, it should be noted that due to the greater homogeneity of the profile in the case of an oscillatory strategy, a higher maximum effective height is obtained in a wall with a maximum value of measured height lower than that observed in the case of an overlapping strategy.

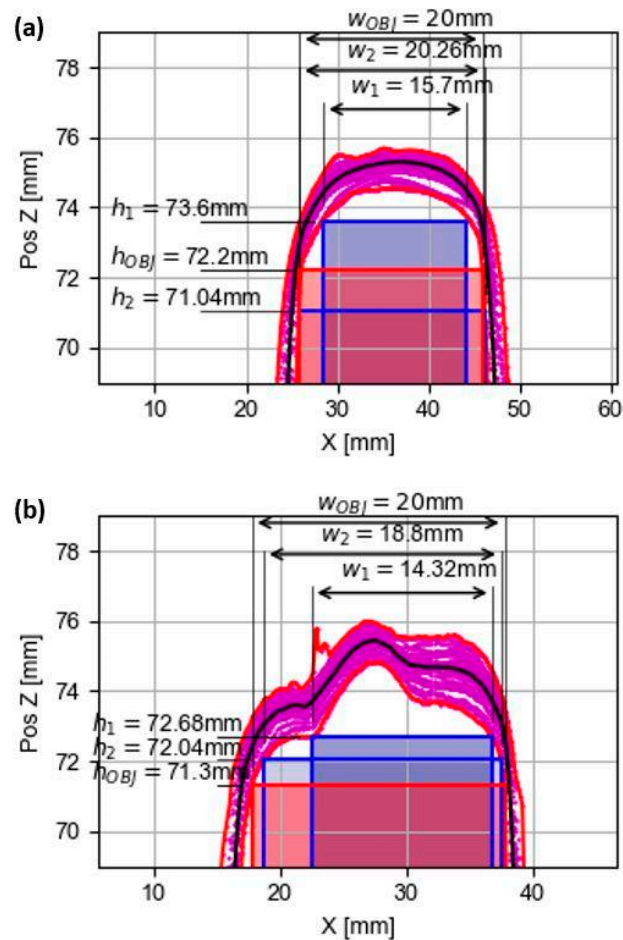


Figure 15. Calculation of the effective cross-sectional area of the wall manufactured by means of (a) oscillating strategy or (b) overlapping of linear welds strategy.

In the following Figure 16, the cross-sectional area value is shown considering the rectangular wall section. This area is calculated as the effective height value for the different wall widths that can be obtained with both strategies. The oscillatory strategy allows better use of the material provided due to the greater homogeneity of the measured profile, even finding Z-level values, corresponding to the height, in the case of the overlapping strategy. In general, this produces a greater effective cross-sectional area in the case of an oscillatory strategy, in addition to a smaller volume of shavings removed to obtain the final wall. This fact entails a lower cost in subsequent machining processes.

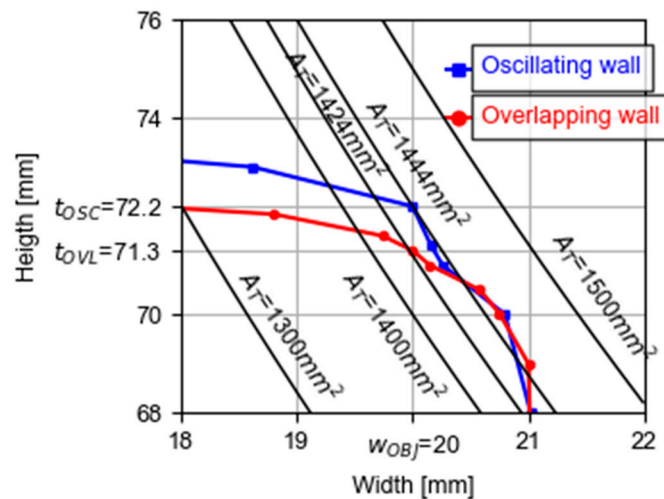


Figure 16. Calculation of the effective cross-sectional area of the wall manufactured according to the effective height and width in the different manufacturing strategies.

4. Conclusions

Low-carbon steel (ER70S-6) walls were manufactured with the GMAW-WAAM technique. The oscillatory and overlapping strategies were used and compared in the fabrication of 20 mm × 70 mm × 220 mm walls. Different process aspects and parameters were compared to illustrate a clear idea of the advantages and disadvantages of each one. The main aspects studied were the material deposition, the growth per layer, the heat input, the fabrication time, the microstructure, the mechanical properties and the wall geometry. Some conclusions drawn from this comparison are:

- In this paper, two manufacturing strategies have been evaluated in terms of geometry and mechanical properties (tensile strength, hardness and Charpy). Similar mechanical values and manufacturing times have been observed. The manufacture of parts with different and complementary strategies increases the adaptation of technology to complex geometries, allowing the application in parts that have crossings, variable wall thickness or curvature.
- The non-productive idle time establishes the differences observed on productivity in each case. The cooling time (part of the idle time where the wall is at rest until it reaches the desired temperature) is lower in the oscillated wall. The oscillated wall consists of a continuous trajectory on each layer; on the other hand, the overlapping strategy requires three discrete trajectories to cover the same width. After each of these beads, a stop must be made. Therefore, this waste of time makes the overlapping strategy less attractive from a productivity point of view.
- The tensile tests show similar data in both strategies, but certain differences derived from their operating principle can be concluded. Although the Yield Strength and UTS are slightly higher in the case of overlapping trajectory, the elongation before breakage is less. Besides this undesired behavior observed during its elongation, it is observed that the extraction direction of the specimen affects the measured elongation. In the case of the overlapping wall, the specimens in the vertical direction show lower elongation values than those shown in the horizontal direction. The oscillatory strategy presents more homogeneous values in both directions due to the more homogeneous distribution of the beads.
- Mechanical properties were tested, and similar hardness measured in both strategies were obtained. Large variation associated with anisotropy of the material deposition and heating cycles is observed on the measured hardness. Regarding the impact study, Charpy testing shows similar results on both the overlapping and oscillating strategies.

- The flatness in the upper layer is improved thanks to the use of the oscillatory strategy. In the wall made by overlapping, a greater growth of the middle wall is observed, which worsens the flatness values. This fact affects the surface finishing process, from additive surface to finished surface.
- Finally, the analysis of wall geometry is important because it determines the achieved effective wall geometry and it has an influence on the final part machining. The oscillating wall presents improved flatness, and it is quasi-symmetrical, obtaining a greater homogeneity. Using the oscillatory strategy allows better use of material, achieving a lower cost in subsequent machining. Further studies must be done to evaluate the influence of overlapping distance and frequency in the case oscillating strategies.

Author Contributions: Conceptualization, F.V., A.S., and E.A.; data curation, F.V., A.S., and E.A.; formal analysis, F.V., A.L., and E.A.; investigation, F.V., A.S., and E.A.; methodology, F.V. and E.A.; project administration, A.S., A.L.; supervision, A.S. and J.B.; validation, A.L. and A.S.; writing—original draft, F.V. and A.L.; writing—review and editing, F.V., J.B., A.S., and E.A. All authors have read and agreed to the published version of the manuscript.

Funding: The authors acknowledge the Basque Government for financing the PROCODA project, ELKARTEK 2019 program (KK-2019/00004) and HARIPLUS project, HAZITEK 2019 program (ZL-2019/00352) and to the European commission through EiT Manufacturing programme in DEDALUS project (reference ID 20094).

Conflicts of Interest: The authors declare no conflict of interest.

References

1. Frazier, W.E. Metal additive manufacturing: A review. *J. Mater. Eng. Perform.* **2014**, *23*, 1917–1928. [[CrossRef](#)]
2. ASTM International. F2792-12a—Standard terminology for additive manufacturing technologies. *Rapid Manuf. Assoc.* **2013**, 10–12. [[CrossRef](#)]
3. ISO/ASTM52900-15, *Standard Terminology for Additive Manufacturing—General Principles—Terminology*; ASTM International: Conshohocken, PA, USA, 2015. [[CrossRef](#)]
4. Ding, D.; Pan, Z.; Cuiuri, D.; Li, H. Wire-feed additive manufacturing of metal components: Technologies, developments and future interests. *Int. J. Adv. Manuf. Technol.* **2015**, *81*, 465–481. [[CrossRef](#)]
5. Jin, W.; Zhang, C.; Jin, S.; Tian, Y.; Wellmann, D.; Liu, W. Wire arc additive manufacturing of stainless steels: A review. *Appl. Sci.* **2020**, *10*, 1563. [[CrossRef](#)]
6. Wang, L.; Xue, J.; Wang, Q. Correlation between arc mode, microstructure, and mechanical properties during wire arc additive manufacturing of 316L stainless steel. *Mater. Sci. Eng. A* **2019**, *751*, 183–190. [[CrossRef](#)]
7. Derekar, K.S. A review of wire arc additive manufacturing and advances in wire arc additive manufacturing of aluminium. *Mater. Sci. Technol.* **2018**, *34*, 895–916. [[CrossRef](#)]
8. Williams, S.; Martina, F.; Addison, A.C.; Ding, J.; Pardal, G.; Colegrove, P. Wire + arc additive manufacturing. *Mater. Sci. Technol.* **2016**, *32*, 641–647. [[CrossRef](#)]
9. Xu, X.; Ding, J.; Ganguly, S.; Diao, C.; Williams, S. Preliminary investigation of building strategies of maraging steel bulk material using wire + arc additive manufacture. *J. Mater. Eng. Perform.* **2018**, *28*, 594–600. [[CrossRef](#)]
10. Chen, Y.; He, Y.; Chen, H.; Zhang, H.; Chen, S. Effect of weave frequency and amplitude on temperature field in weaving welding process. *Int. J. Adv. Manuf. Technol.* **2014**, *75*, 803–813. [[CrossRef](#)]
11. Taberero, I.; Paskual, A.; Álvarez, P.; Suárez, A. Study on arc welding processes for high deposition rate additive manufacturing. *Procedia CIRP* **2018**, *68*, 358–362. [[CrossRef](#)]
12. Selvi, S.; Vishvakshnan, A.; Rajasekar, E. Cold metal transfer (CMT) technology—An overview. *Def. Technol.* **2018**, *14*, 28–44. [[CrossRef](#)]
13. Dinovitzer, M.; Chen, X.; Laliberte, J.; Huang, X.; Frei, H. Effect of wire and arc additive manufacturing (WAAM) process parameters on bead geometry and microstructure. *Addit. Manuf.* **2019**, *26*. [[CrossRef](#)]
14. Rios, S.; Colegrove, P.; Martina, F.; Williams, S. Analytical process model for wire + arc additive manufacture. *Addit. Manuf.* **2018**, *21*. [[CrossRef](#)]
15. Dirasu, P.; Ganguly, S.; Mehmanparast, A.; Martina, F.; Williams, S. Analysis of fracture toughness properties of wire + arc additive manufactured high strength low alloy structural steel components. *Mater. Sci. Eng. A* **2019**, *765*, 138285. [[CrossRef](#)]
16. Kah, P.; Suoranta, R.; Martikainen, J. Advanced gas metal arc welding processes. *Int. J. Adv. Manuf. Technol.* **2013**, *67*, 655–674. [[CrossRef](#)]

17. Salmi, M.; Huuki, J.; Flores, I. The ultrasonic burnishing of cobalt-chrome and stainless steel surface made by additive manufacturing. *Prog. Addit. Manuf.* **2017**, *2*, 31–41. [[CrossRef](#)]
18. MacKenzie, D.; Totten, G. *Analytical Characterization of Aluminum, Steel, and Superalloys*; CRC Press: Boca Raton, FL, USA, 2006. [[CrossRef](#)]
19. Metallic Materials—Tensile Testing—Part 1: Method of Test at Room Temperature, Geneva, Switzerland, 2019, ISO 6892-1:2019. Available online: <https://www.iso.org/standard/78322.html> (accessed on 31 May 2020).
20. Ghaffari, M.; Vahedi Nemani, A.; Rafieazad, M.; Nasiri, A. Effect of solidification defects and HAZ softening on the anisotropic mechanical properties of a wire arc additive-manufactured low-carbon low-alloy steel part. *J. Miner. Met. Mater. Soc.* **2019**, *71*, 4215–4224. [[CrossRef](#)]
21. Gordon, J.V.; Vinci, R.P.; Hochhalter, J.D.; Rollett, A.D.; Harlow, D.G. Quantification of location-dependence in a large-scale additively manufactured build through experiments and micromechanical modeling. *Materialia* **2019**, *7*, 100397. [[CrossRef](#)]
22. Choi, C.L.; Hill, D.C. A study of microstructural progression in as-deposited weld metal. *Weld. J.* **1978**, *57*, 232.
23. Babu, S.S. The mechanism of acicular ferrite in weld deposits. *Curr. Opin. Solid State Mater. Sci.* **2004**, *8*, 267–278. [[CrossRef](#)]
24. Grong, O.; Matlock, D.K. Microstructural development in mild and low-alloy steel weld metals. *Int. Met. Rev.* **1986**, *31*, 27–48. [[CrossRef](#)]
25. Ma, G.; Zhao, G.; Li, Z.; Yang, M.; Xiao, W. Optimization strategies for robotic additive and subtractive manufacturing of large and high thin-walled aluminum structures. *Int. J. Adv. Manuf. Technol.* **2019**, *101*, 1275–1292. [[CrossRef](#)]
26. Bai, X.; Colegrove, P.; Ding, J.; Zhou, X.; Diao, C.; Bridgeman, P.; Hönnige, J.R.; Zhang, H.; Williams, S. Numerical analysis of heat transfer and fluid flow in multilayer deposition of PAW-based wire and arc additive manufacturing. *Int. J. Heat Mass Transf.* **2018**, *124*, 504–516. [[CrossRef](#)]
27. Veiga, F.; Gil Del Val, A.; Suárez, A.; Alonso, U. Analysis of the machining process of titanium Ti6Al-4V parts manufactured by wire arc additive manufacturing (WAAM). *Materials* **2020**, *13*, 766. [[CrossRef](#)] [[PubMed](#)]



© 2020 by the authors. Licensee MDPI, Basel, Switzerland. This article is an open access article distributed under the terms and conditions of the Creative Commons Attribution (CC BY) license (<http://creativecommons.org/licenses/by/4.0/>).